Radiation Report

INA1H94-SEP Single-Event Effects (SEE) Radiation Report

ABSTRACT

Studies were performed to characterize the effects of heavy-ion irradiation on the single-event latch-up (SEL) performance of the INA1H94-SEP radiation-tolerant, high common-mode voltage difference amplifier. For device qualification, heavy ions with an LET_{EFF} of 45.9MeV-cm^2 / mg were used to irradiate the devices with a fluence of 1 × 10^7 ions / cm^2. The results demonstrated that the INA1H94-SEP is SEL-free up to the specified surface LET_{EFF} = 43MeV-cm^2/ mg at 125°C.

Characterization of single-event transients (SET) and correlation testing of SEL were also performed, up to a surface LET_{EFF} = 45.9MeV-cm^2/ mg at 125°C.

Table of Contents

1 Overview....2
2 SEE Mechanisms....3
3 Irradiation Facilities and Telemetry....3
4 Test Device and Test Board Information....3
4.1 Qualification Circuits and Boards....4
4.2 Characterization Devices and Test Board Schematics....5
5 Results....7
5.1 SEL Qualification Results....7
5.2 SET Characterization Results: TAMU K500 Cyclotron....11
5.3 Analysis....13
6 Summary....14
A Texas A&M University Results Appendix....15
B References....18

Trademarks

All trademarks are the property of their respective owners.

Copyright © 2025 Texas Instruments Incorporated

1 Overview

The INA1H94-SEP is a radiation-tolerant precision unity-gain difference amplifier with a very high input common-mode voltage range. The INA1H94-SEP is a single, monolithic device that consists of a precision op amp and an integrated thin-film resistor network. The INA1H94-SEP can accurately measure small differential voltages in the presence of common-mode signals up to ±150V. In many applications where galvanic isolation is not required, the INA1H94-SEP can replace isolation amplifiers. The excellent 0.0005% typical nonlinearity, high common mode, and 500kHz bandwidth of the INA1H94-SEP makes for a compelling sensor readout device. This device runs on a single 4V to 18V supply or dual ±2V to ±9V supplies.

Table 1-1. Overview Information (1)

Description	Device Information
TI Part Number	INA1H94-SEP
DLA VID	V62/25652
Device Function	INA1H94-SEP Radiation-Tolerant, High Common-Mode Voltage Difference Amplifier
Fab Technology	BICMOS
Fab Process	BICOM-3XHV
Exposure Facilities	Single Event Effects Facility, Cyclotron Institute, Texas A&M University
Heavy Ion Fluence per Run	1×10^7 ions/cm^2
Irradiation Temperature	125°C (for SEL testing) And 25°C (for SET testing)

(1) TI may provide technical, applications or design advice, quality characterization, and reliability data or service, providing these items shall not expand or otherwise affect TI's warranties as set forth in the Texas Instruments Incorporated Standard Terms and Conditions of Sale for Semiconductor Products and no obligation or liability shall arise from Semiconductor Products and no obligation or liability shall arise from TI's provision of such items.

Copyright © 2025 Texas Instruments Incorporated

2 SEE Mechanisms

The primary single-event effect (SEE) of interest in the INA1H94-SEP is single-event latch-up (SEL). From a risk and potential impact point-of-view, the occurrence of an SEL is possibly the most destructive SEE event and the biggest concern for space applications. A BICMOS process node was used for the INA1H94-SEP, though the device is primarily bipolar. CMOS circuitry often introduces a potential for SEL susceptibility. SEL can occur if excess current injection caused by the passage of an energetic ion is high enough to trigger the formation of a parasitic cross-coupled PNP and NPN bipolar structure (formed between the p-sub and n-well and n+ and p+ contacts). The parasitic bipolar structure initiated by a single-event creates a high-conductance path (inducing a steady-state current that is typically orders of magnitude higher than the normal operating current) between power and ground that persists (is *latched*) until the power is removed or until the device is destroyed by the high-current state.

The INA1H94-SEP is specified as SEL-free to a surface LET_{EFF} of 43MeV-cm^2/ mg, at a fluence of 10^7 ions / cm^2 and a chip temperature of 125°C. The INA1H94-SEP was shown in characterization to exhibit no SEL with heavy ions up to a surface LET_{EFF} of 45.9MeV-cm^2/ mg, at a fluence of 10^7 ions / cm^2 and a chip temperature of 125°C.

3 Irradiation Facilities and Telemetry

For SEL qualification and SET characterization testing, heavy ion species were provided and delivered by the TAMU Cyclotron Radiation Effects Facility [3] using a superconducting cyclotron and advanced electron cylotorn resonance (ECR) ion source. Ion beams were delivered with high uniformity over a 1-inch diameter circular cross sectional area for the in-air station. Uniformity is achieved by magnetic defocusing. The intensity of the beam is regulated over a broad range spanning several orders of magnitude. These measurements are real-time continuous and establish dosimetry and integrated fluence. An ion flux of 10^5 ions / s-cm^2 was used to provide heavy ion fluences to 10^7 ions / cm^2 for most runs. Ion flux was increaded to 1.5 × 10^7 ions / s-cm^2 for some runs, to show SEL immunity at multiple flux rates and to explore the effect of flux rate on transient event counts.

4 Test Device and Test Board Information

The INA1H94-SEP is packaged in an 8-pin SO package. Figure 4-1 shows the pinout diagram. The package lid was removed to reveal the die face for all heavy ion testing.

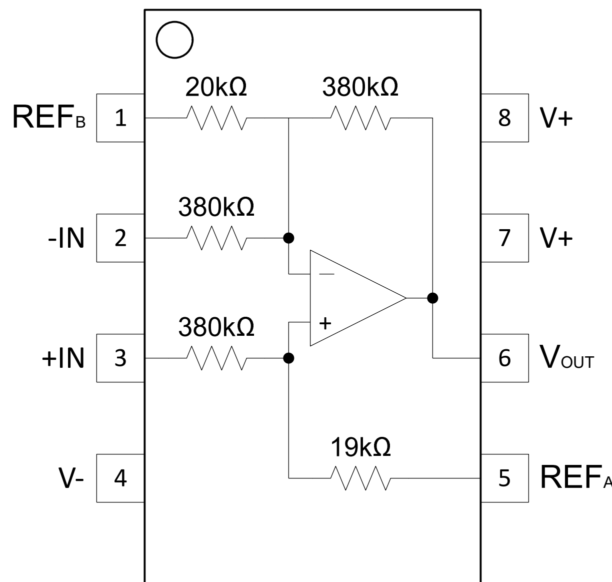

Figure 4-1. INA1H94-SEP Pinout Diagram

Each device under test, or DUT, used for single-event effect qualification and characterization was sourced from the same wafer fab and assembly lot, which was used for all INA1H94-SEP qualification studies. Across the SEL, SET, and absolute-maximum supply extended SEL characterization tests performed, a total of 5 different

Copyright © 2025 Texas Instruments Incorporated

devices were evaluated. Some lookahead testing was also performed on units from different assembly lots, with no significant differences observed in the test results.

4.1 Qualification Circuits and Boards

The INA1H94-SEP was biased in a variety of different conditions for SEE testing, at both the recommended minimum and recommended maximum supply voltages. Midsupply or GND was used for both REF_A and REF_B. Current was monitored over time for both supplies V+, V- and the instrumentation amplifier inputs -IN and +IN.

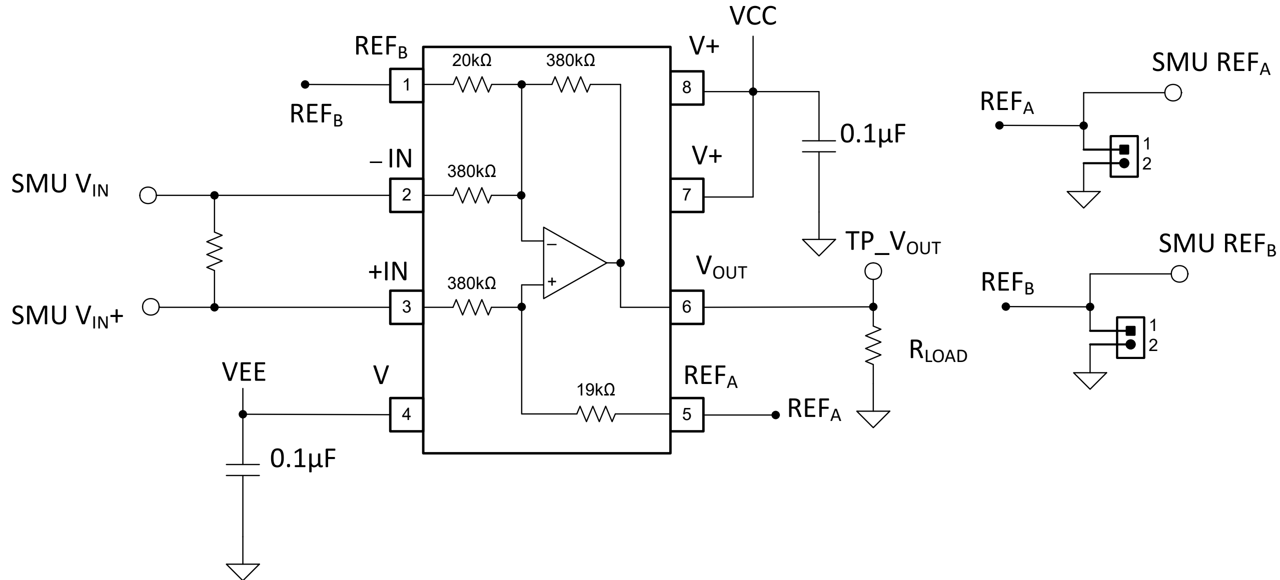

Figure 4-2. INA1H94-SEP SEE Qualification Bias Diagram

Input and supply voltages were provided by SMU PXI cards, connected with banana cables. The board used for testing incorporated jumpers to allow testing with high V_{CM} and 0V V_{DIFF}; low V_{CM} and high V_{DIFF}; and high V_{CM} and constant V_{DIFF}. For all testing, the device outputs were monitored using oscilloscope PXI cards, connected with BNC cables. A 100Ω of series isolation resistance was used to drive the cable capacitance. A 2kΩ output load to midsupply was present for all DUTs.

An example of the INA1H94-SEP device mounted through a socket on a characterization board is shown in Figure 4-3. During SEL qualification, the device was heated using forced hot air, maintaining an IC temperature at 125°C. During SEL testing, the devices were soldered into a coupon board, allowing direct airflow access to the heater. For SET testing, devices were mounted in a socket for the easy exchange of units.

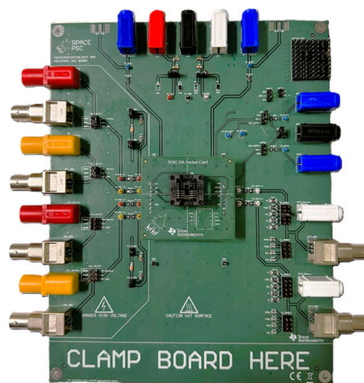

Figure 4-3. Characterization Board

Copyright © 2025 Texas Instruments Incorporated

4.2 Characterization Devices and Test Board Schematics

Heavy ions were used to irradiate the devices. A nominal flux of 1.3×10^5 ions / s-cm^2 was used for SEL characterization, at 125°C die temperature. Nominal flux of 1×10^5 ions / s-cm^2 was used for SET characterization, at ambient temperature.

For SEE characterization, the INA1H94-SEP was biased with bipolar split supplies. The circuit was connected as shown on Figure 4-4. Different supply voltages, input common-mode voltages and differential voltage conditions were tested.

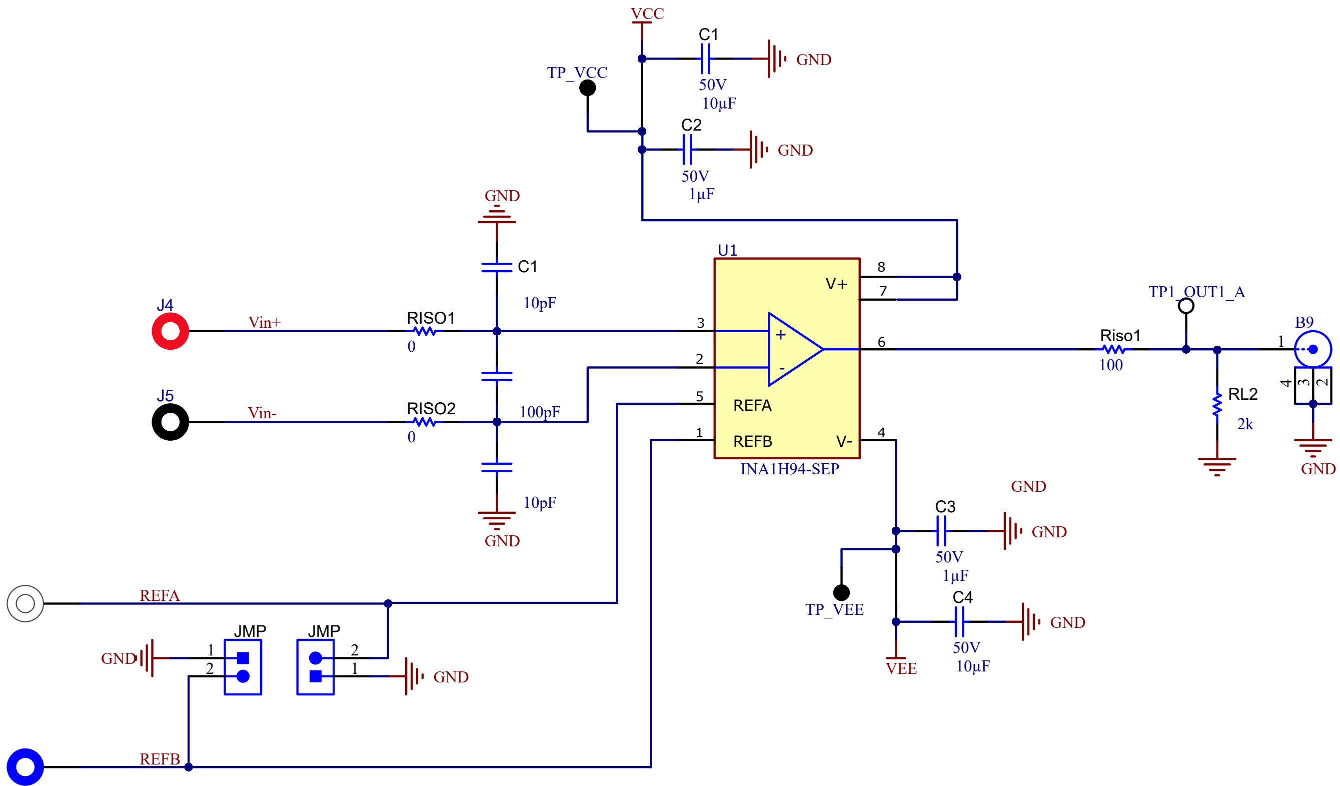

Figure 4-4. SEE Characterization Circuit Block Diagram

Input and supply voltages were provided by SMU PXI cards, connected with banana cables. Figure 4-5 shows the decoupling supply capacitance scheme used. Current was monitored over time for both V+ and V-.

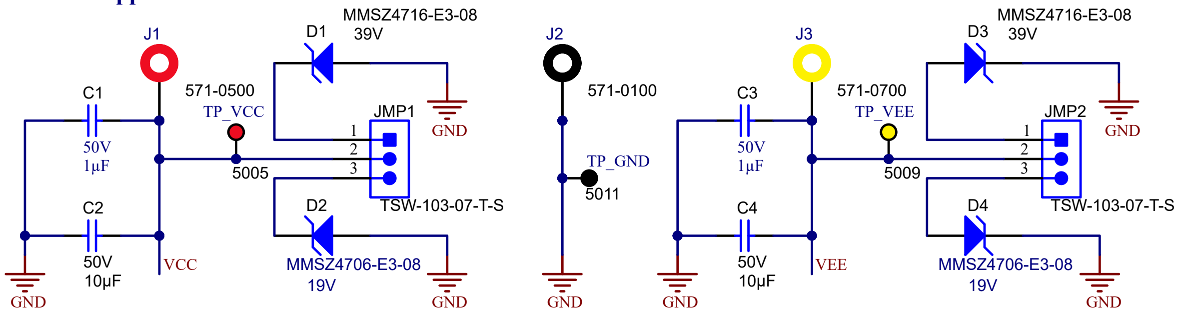

Figure 4-5. Characterization Board Voltage Supply Connections

The positive and negative inputs of the difference amplifier are driven with separate SMU sources, allowing control of the differential and common-mode voltage input signals.Figure 4-5 shows the input SMU connections and optional filters.

Copyright © 2025 Texas Instruments Incorporated

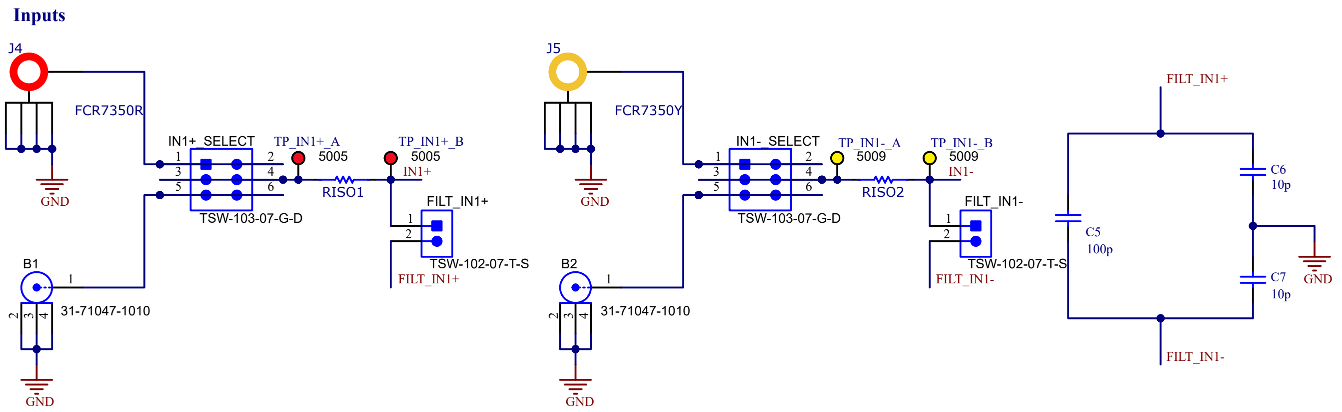

Figure 4-6. Characterization Board Input Connections

For SET testing, the device outputs were monitored using oscilloscope PXI cards, connected with BNC cables. 100Ω of series isolation resistance was used on the output channel to drive the cable capacitance. Figure 4-5 shows the output oscilloscope connections and optional load resistors and capacitors.

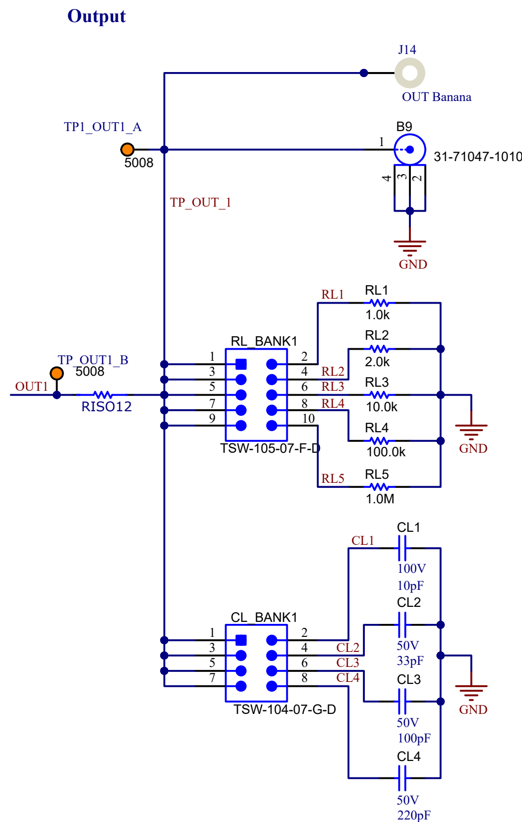

Figure 4-7. Characterization Board Output Connections

Copyright © 2025 Texas Instruments Incorporated

5 Results

5.1 SEL Qualification Results

During SEL qualification, the device was heated using forced hot air, maintaining an IC temperature at 125°C. The temperature was monitored using a thermal camera. The species used for the SEL testing was a silver (^{109}Ag) ion with an angle-of-incidence of 0° and an air gap of 27.7mm, for an LET_{EFF} = 45.9MeV-cm^2/mg. A nominal flux of 10^5 ions / s-cm^2 and fluence of 10^7 ions / cm^2 were targeted for each run. A total of three different DUTs were used for this testing, together experiencing a cumulative total fluence of approximately 29.1× 10^7 ions / cm^2 with no failures observed.

An exhaustive summary of the conditions for the 3 SEL test runs performed is provided in Table 5-1. The run numbers listed are the actual run numbers from the testing session, and the flux, fluence, and dose in silicon for each run are pulled from the test session log provided by the Cyclotron Institute, at Texas A&M University. Figure 5-2 and related figures show example plots of the supply currents versus time.

Table 5-1. INA1H94-SEP SEL Testing Summary, ^{109}Ag Ion, 125°C Die Temperature

Run #	DUT	V+ Supply (V)	V- Supply (V)	Input V_{CM} (V)	Input V_{DIFF} (V)	Mean Flux (ions/s-cm^2)	Fluence (ions/cm^2)	Dose in Silicon (Rad)
10	D3	9	-9	155	7.5	1.229×10^5	9.941×10^6	7.311×10^3
11	D3	9	-9	-155	-7.5	1.297×10^5	1.005×10^7	7.392×10^3
12	D3	2.5	-2.5	22.5	1	1.286×10^5	9.961×10^6	7.326×10^3
13	D3	2.5	-2.5	-22.5	-1	1.262×10^5	1.005×10^7	7.391×10^3
14	D3	9	-9	3.75	7.5	1.105×10^5	8.361×10^5	6.149×10^2
15	D3	9	-9	3.75	7.5	1.224×10^5	1.000×10^7	7.358×10^3
16	D3	9	-9	-3.75	-7.5	1.230×10^5	1.005×10^7	7.391×10^3
17	D3	2.5	-2.5	0.5	1	1.260×10^5	1.499×10^7	1.103×10^4
18	D3	2.5	-2.5	-0.5	-1	1.271×10^5	1.501×10^7	1.104×10^4
19	D4	9	-9	155	7.5	1.403×10^5	1.006×10^7	7.395×10^3
20	D4	9	-9	-155	-7.5	1.330×10^5	1.000×10^7	7.355×10^3
21	D4	2.5	-2.5	22.5	1	1.268×10^5	9.982×10^6	7.341×10^3
22	D4	2.5	-2.5	-22.5	-1	1.238×10^5	1.002×10^7	7.368×10^3
23	D4	9	-9	3.75	7.5	1.173×10^5	1.002×10^7	7.371×10^3
24	D4	9	-9	-3.75	-7.5	1.212×10^5	9.994×10^6	7.350×10^3
25	D4	2.5	-2.5	0.5	1	1.118×10^5	9.943×10^6	7.313×10^3
26	D4	2.5	-2.5	-0.5	-1	1.161×10^5	9.965×10^6	7.329×10^3
27	D5	9	-9	155	7.5	1.290×10^5	9.998×10^6	7.353×10^3
28	D5	9	-9	155	-7.5	7.820×10^4	1.681×10^5	1.237×10^2
29	D5	9	-9	155	-7.5	1.239×10^5	9.989×10^6	7.346×10^3
30	D4	2.5	-2.5	22.5	1	1.323×10^5	1.006×10^7	7.402×10^3
31	D4	2.5	-2.5	-22.5	-1	1.193×10^5	1.004×10^7	7.383×10^3
32	D4	9	-9	3.75	7.5	1.184×10^5	1.001×10^7	7.358×10^3
33	D4	9	-9	3.75	7.5	1.149×10^5	1.003×10^7	7.377×10^3
34	D4	9	-9	-3.75	-7.5	1.106×10^5	9.899×10^6	7.347×10^3
35	D4	2.5	-2.5	0.5	1	1.142×10^5	1.002×10^7	7.367×10^3
36	D4	2.5	-2.5	-0.5	-1	1.132×10^5	1.006×10^7	7.395×10^3

Copyright © 2025 Texas Instruments Incorporated

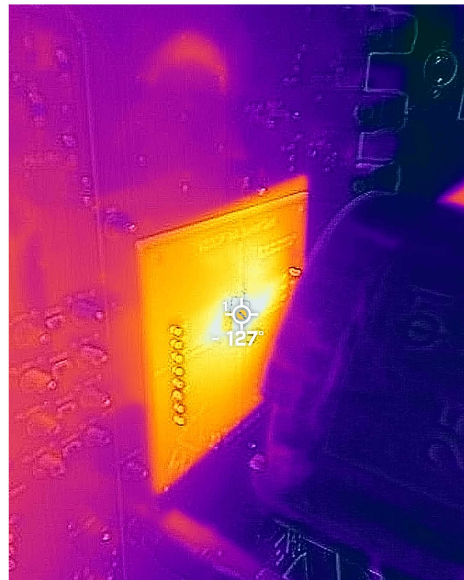

Figure 5-1. Thermal Image During Set Up

No SEL events were observed, which indicates that the INA1H94-SP is SEL-immune at LET_{EFF} = 45.9MeV-cm^2/mg and T = 125°C. Using the MFTF method described in Confidence Interval Calculations and combining (or summing) the fluences of the two runs at 125°C (2 × 10^7), the upper-bound cross-section (using a 95% confidence level) is calculated in Equation 1:

$\sigma SEL \leq 1.84 \times 10^{-7}$ cm^2 for LET_{EFF} = 45.9MeV-cm^2/ mg and T = 125°C.

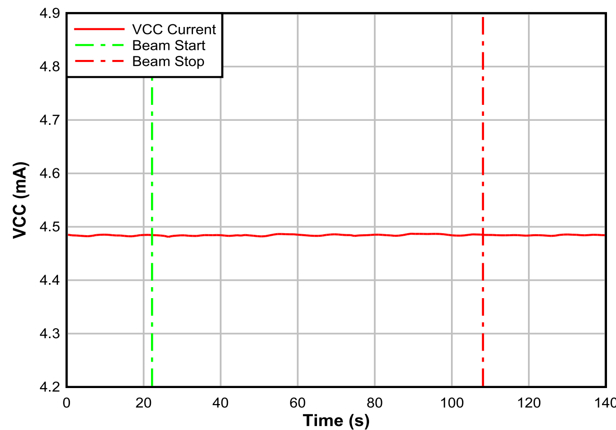

Figure 5-2. Current Versus Time (I Versus t) Data for V+ Current During SEL Run 15

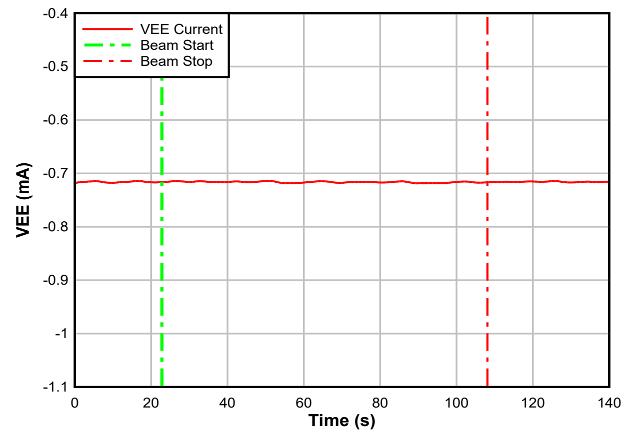

Figure 5-3. Current Versus Time (I Versus t) Data for V- Current During SEL Run 15

Copyright © 2025 Texas Instruments Incorporated

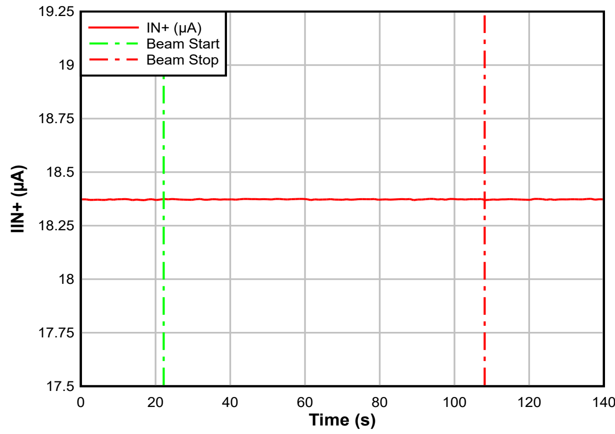

Figure 5-4. Current Versus Time (I Versus t) Data for I_{IN+} Current During SEL Run 15

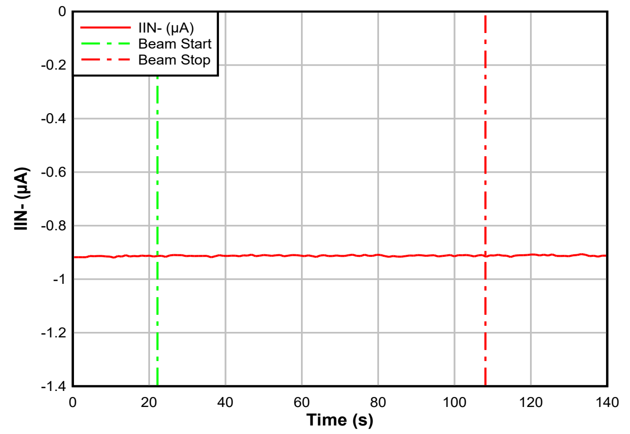

Figure 5-5. Current Versus Time (I Versus t) Data for I_{IN-} Current During SEL Run 15

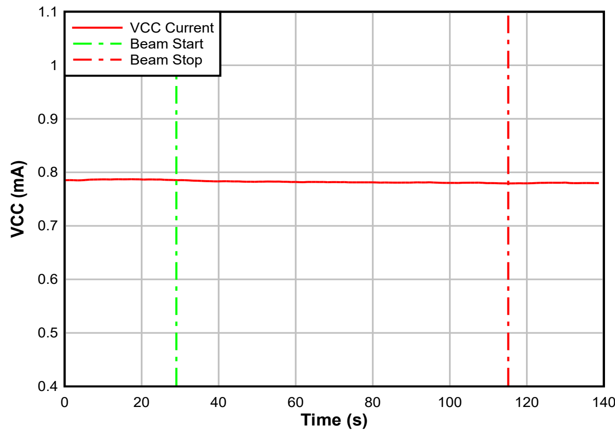

Figure 5-6. Current Versus Time (I Versus t) Data for V+ Current During SEL Run 22

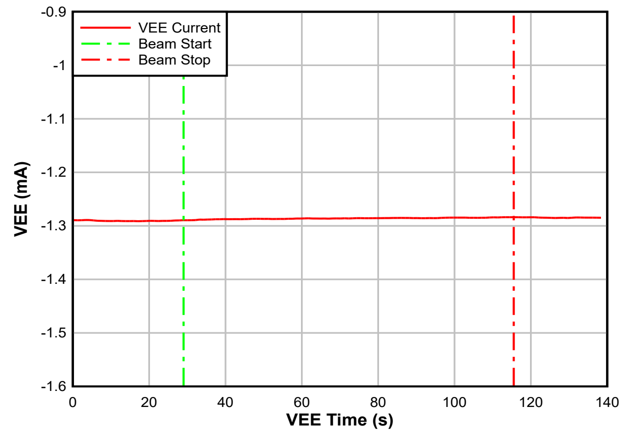

Figure 5-7. Current Versus Time (I Versus t) Data for V- Current During SEL Run 22

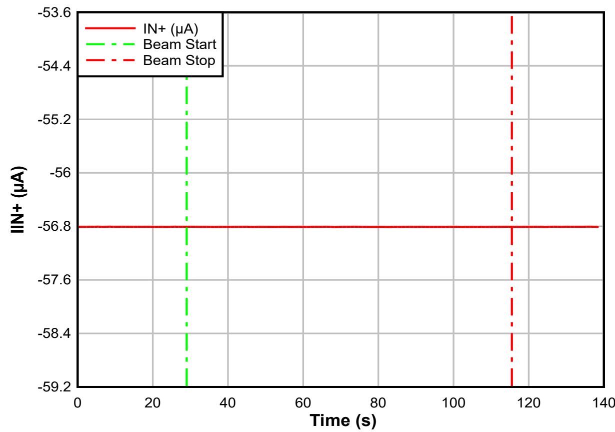

Figure 5-8. Current Versus Time (I Versus t) Data for I_{IN+} Current During SEL Run 22

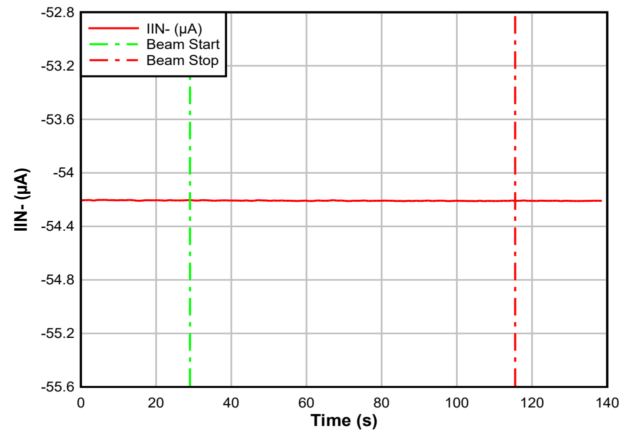

Figure 5-9. Current Versus Time (I Versus t) Data for I_{IN-} Current During SEL Run 22

Copyright © 2025 Texas Instruments Incorporated

Additional tests were performed on unit D4 at the absolute maximum supply of 24V at LET_{EFF} = 45.9MeV-cm^2/mg and T = 125°C without any failures observed. A summary of the conditions in test runs performed is provided in Table 5-2.

Table 5-2. INA1H94-SEP SEL Test Summary at absolute maximum supply, ^{109}Ag Ion, 125°C Die Temperature

Run #	DUT	V+ Supply (V)	V- Supply (V)	Input V_{CM} (V)	Input V_{DIFF} (V)	Mean Flux (ions × cm^2/mg)	Fluence (ions/cm^2)	Dose in Silicon (rad)
37	D4	12	-12	1	2	1.132×10^5	9.952×10^6	7.319×10^3
38	D4	12	-12	-1	-2	1.214×10^5	9.947×10^6	7.315×10^3
39	D4	12	-12	155	7	1.266×10^5	9.985×10^6	7.344×10^3

Copyright © 2025 Texas Instruments Incorporated

5.2 SET Characterization Results: TAMU K500 Cyclotron

Three fresh DUTs were used for SET characterization. The conditions for each run are summarized on Table 5-3 below.

The device was tested at maximum specified supply voltage range of ±9V (or 18V total supply) and input common mode voltage (V_{CM}) of ±150V with a fixed input differential voltage V_{DIFF}. he REFA and REFB pins were biased at mid-supply (0V). The device output channel was loaded with a 2kΩ resistance to GND (midsupply). Tests were repeated at the lower specified supply voltage range of ±2.5V (or 5V total supply) with V_{CM} =±22.5V.

The oscilloscopes were set to a *window* trigger mode that captured any events where the output shifted by ±100mV or more.

The devices were exposed to LET levels varying from 45.9MeV-cm^2 / mg to 8.83MeV-cm^2 / mg. An ambient temperature of approximately 25°C was recorded in the facility at the time of these tests. See Appendix A for additional data, such as histograms.

Runs 2, 18 from the session are excluded on the table. These runs were interrupted due to set up adjustments. However, the same DUT test conditions were repeated in the following run.

Table 5-3. TAMU SET Characterization Run Summary

Run Number	DUT	Supply (V)	V_{DIFF} (V)	V_{CM} (V)	Ion	LETeff (MeV-cm^2/mg)	Flux (ions/s-cm^2)	Fluence (ions/cm^2)	Total Ionizing Dose (rad)	Events
1	SET1	±2.5	0.5	20	^{109}Ag	45.9	1.382×10^5	1.003×10^7	7.205E+03	13008
3	SET1	±2.5	-0.5	-20	^{109}Ag	45.9	1.375×10^5	9.993×10^6	7.349×10^3	14069
4	SET1	±9	3.5	150	^{109}Ag	45.9	1.279×10^5	9.940×10^6	7.310×10^3	11367
5	SET1	±9	-3.5	-150	^{109}Ag	45.9	1.309×10^5	1.003×10^7	7.374×10^3	8090
6	SET2	±2.5	0.5	20	^{109}Ag	45.9	1.299×10^5	9.993×10^6	7.343×10^3	12306
7	SET2	±2.5	-0.5	-20	^{109}Ag	45.9	1.298×10^5	9.950×10^6	7.318×10^3	14230
8	SET2	±9	3.5	150	^{109}Ag	45.9	1.262×10^5	1.004×10^7	7.383×10^3	11830
9	SET2	±9	-3.5	-150	^{109}Ag	45.9	1.256×10^5	9.995×10^6	7.351×10^3	8340
16	SET1	±2.5	0.5	20	^{84}Kr	34.5	1.101×10^5	1.003×10^7	8.762×10^3	9814
17	SET1	±2.5	-0.5	20	^{84}Kr	34.5	1.001×10^5	1.002×10^7	8.751×10^3	10020
19	SET1	±9	3.5	150	^{84}Kr	34.5	9.232×10^4	1.000×10^7	8.737×10^3	10165
20	SET1	±9	-3.5	-150	^{84}Kr	34.5	8.802×10^4	9.975×10^6	8.714×10^3	11164
21	SET1	±2.5	0.5	20	^{84}Kr	29.1	1.233×10^5	9.974×10^6	7.126×10^3	9179
22	SET1	±2.5	-0.5	-20	^{84}Kr	29.1	8.793×10^4	9.992×10^6	7.139×10^3	10368
23	SET1	±9	3.5	150	^{84}Kr	29.1	8.066×10^4	9.993×10^6	7.140×10^3	10104
24	SET1	±9	-3.5	-150	^{84}Kr	29.1	7.839×10^4	9.980×10^6	7.130×10^3	10993
25	SET1	±2.5	0.5	20	^{63}Cu	19.3	9.994×10^4	9.976×10^6	4.744×10^3	9376
26	SET1	±2.5	-0.5	-20	^{63}Cu	19.3	9.738×10^4	9.977×10^6	4.745×10^3	9530
27	SET1	±9	3.5	150	^{63}Cu	19.3	1.055×10^5	1.002×10^7	4.764×10^3	9310
28	SET1	±9	-3.5	-150	^{63}Cu	19.3	9.960×10^4	9.965×10^6	4.739×10^3	9564
29	SET1	±2.5	0.5	20	^{15}Ar	8.83	1.028×10^5	9.977×10^6	1.996×10^3	6940
30	SET1	±2.5	-0.5	-20	^{15}Ar	8.83	9.127×10^4	1.001×10^7	2.001×10^3	6997
31	SET1	±9	3.5	150	^{15}Ar	8.83	1.093×10^5	9.998×10^6	2.000×10^3	7436
32	SET1	±9	-3.5	-150	^{15}Ar	8.83	1.108×10^5	1.003×10^7	2.006×10^3	7647

Additional follow-up testing was performed on a second session at TAMU. For these tests, lower-energy ions were used, to determine the transient onset point. Measurements at 2.73MeV-cm2 / mg, and 1.33MeV-cm2 / mg were explored. The test conditions previously described were replicated for these runs.

Copyright © 2025 Texas Instruments Incorporated

Table 5-4. TAMU SET Follow-up Characterization Run Summary

Run Number	DUT	Supply (V)	V_{DIFF} (V)	V_{CM} (V)	Ion	LETeff (MeV-cm^2/mg)	Flux (ions/s-cm^2)	Fluence (ions/cm^2)	Total Ionizing Dose (rad)	Events
39	SET1	±9	3.5	150	^{20}Ne	2.73	$1.302{\times}10^5$	$9.984{\times}10^6$	$4.632{\times}10^2$	1364
40	SET1	±9	-3.5	-150	^{20}Ne	2.73	$1.272{\times}10^5$	$9.944{\times}10^6$	$4.344{\times}10^2$	2115
41	SET1	±2.5	0.5	20	^{20}Ne	2.73	$1.270{\times}10^5$	$9.993{\times}10^6$	$4.366{\times}10^2$	2115
42	SET1	±2.5	-0.5	-20	^{20}Ne	2.73	$1.281{\times}10^5$	$1.005{\times}10^7$	$4.391{\times}10^2$	2143
43	SET1	±9	3.5	150	^{14}N	1.33	$1.023{\times}10^5$	$1.003{\times}10^7$	$2.132{\times}10^2$	119
44	SET1	±9	3.5	150	^{14}N	1.33	$9.740{\times}10^4$	$9.971{\times}10^6$	$2.121{\times}10^2$	171
45	SET1	±2.5	0.5	20	^{14}N	1.33	$1.088{\times}10^5$	$9.963{\times}10^6$	$2.119{\times}10^2$	154
46	SET1	±2.5	-0.5	-20	^{14}N	1.33	$1.021{\times}10^5$	$9.952{\times}10^6$	$2.117{\times}10^2$	157

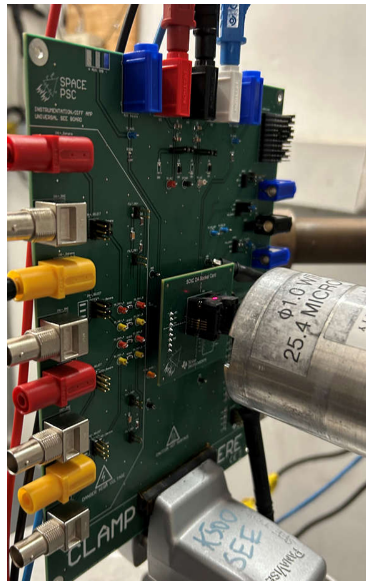

Figure 5-10. Device Under Test Lined Up With the Beam

Copyright © 2025 Texas Instruments Incorporated

5.3 Analysis

Information in this section describes general characteristics of the SET response characteristics of the device, and may not be accurate for all use cases or conditions. In-circuit results vary according to application specifics. TI's customers are responsible for determination of components for their purposes, and validating and testing design implementation to confirm system functionality.

The data suggest the rate at which the INA1H94-SEP exhibits SET events, and the magnitude of those events, is a function of several factors. These include supply voltage, input common-mode voltage (V_{CM}), differential input voltage (V_{DIFF}) beam flux, ion energy, and temperature.

Generally, when the INA1H94-SEP experiences an SET, the device output presents sudden *spikes* and are usually resolved within 10µs of the trigger event. Events where the output shifted by more than ±100mV were recorded by the oscilloscope cards. A small percentage of these captures show measurable undershoot or overshoot behavior after the initial spike as the output settles. Table 5-5 shows notable oscilloscope captures.

Note that the INA1H94-SEP also experiences transient events of less than 100mV. As a result, this study focuses on only events more than 100mV in magnitude. Testing at Texas A&M University has shown that the beam area is an electrically noisy environment, which can lead to false trigger events. As a result, this study focuses on only events more than 100mV in magnitude. Implementing filters on the device to reject noise can lead to reductions in SET count or impact the magnitude of those events.

Device SET1 was evaluated with ion energy in *descending* order, from 45.9MeV-cm^2 / mg to 1.33MeV-cm^2 / mg. This device was evaluated with both positive and negative polarity V_{CM} and V_{DIFF} input voltages.

Device SET2 was evaluated at the higher energy level of 45.9MeV-cm^2 / mg, for verification, providing similar results.

Table 5-5. Sum of Event Counts Per Device

LET (MeV-cm^2 /mg)	Parameter	DUT-SET1		DUT-SET2	
		Vs = 5V	Vs = 18V	Vs = 5V	Vs = 18V
45.9	Events	27077	19457	26536	20170
	Fluence (Ions/cm^2)	2.002E+07	1.997E+07	1.994E+07	2.004E+07
	Cross Section (cm^2)	1.35E-03	7.65E-04	1.33E-03	7.74E-04
34.5	Events	19834	21329	N/A	N/A
	Fluence (Ions/cm^2)	2.005E+07	1.998E+07		
	Cross Section (cm^2)	9.89E-04	1.07E-03		
29.1	Events	19547	21157	N/A	N/A
	Fluence (Ions/cm^2)	1.997E+07	1.997E+07		
	Cross Section (cm^2)	9.79E-04	1.06E-03		
19.3	Events	18906	18874	N/A	N/A
	Fluence (Ions/cm^2)	1.995E+07	1.999E+07		
	Cross Section (cm^2)	9.48E-04	9.44E-04		
8.83	Events	13937	15083	N/A	N/A
	Fluence (Ions/cm^2)	1.999E+07	2.003E+07		
	Cross Section (cm^2)	6.97E-04	7.53E-04		
2.73	Events	4258	3479	N/A	N/A
	Fluence (Ions/cm^2)	2.004E+07	1.993E+07		
	Cross Section (cm^2)	2.12E-04	1.75E-04		
1.33	Events	311	290	N/A	N/A
	Fluence (Ions/cm^2)	1.992E+07	2.000E+07		
	Cross Section (cm^2)	1.56E-05	1.45E-05		

Copyright © 2025 Texas Instruments Incorporated

The INA1H94-SEP susceptibility to SET increases as ion energy level increases. In some cases, differences in readings between devices at similar input voltages can be attributed to differences in the oscilloscope cards used, as verified through A↔B site swaps.

Factors such as the time between decap and testing (time the die is exposed to air), annealing time between runs, and simple device-to-device variation can also play a potential role in the differing event counts. Correlating any single factor to the event counts is difficult due to the complexities and practical challenges of the testing.

Table 5-6. Transient Event Summary for 5V Supply

LET (MeV-cm^2 /mg)	Event Count	Mean Transient Duration (µs)	Std. Dev. Transient Duration (µs)	Avg. Pk. Voltage (V)	Std. Dev. Pk. Voltage (V)	Min. Pk Voltage (V)	Max. Pk Voltage (V)	Mean Abs. Pk. Voltage (V)	Std. Dev. peak Voltage (V)
45.9	20326	1.217	1.190	-0.057	0.617	-1.908	0.980	0.434	0.438
34.5	17196	1.116	0.868	-0.076	0.802	-1.890	1.010	0.677	0.437
29.1	15272	1.110	0.765	-0.101	0.786	-1.868	1.010	0.676	0.415
19.3	11284	1.199	0.600	-0.004	0.531	-1.281	0.986	0.469	0.250
8.83	7905	1.312	0.413	-0.010	0.279	-0.789	0.773	0.261	0.100
2.73	532	1.292	0.386	-0.006	0.194	-0.385	0.379	0.183	0.070
1.33	90	1.266	0.400	-0.005	0.174	-0.237	0.248	0.168	0.052

Table 5-7. Transient Event Summary for 18V Supply

LET (MeV-cm^2 /mg)	Event Count	Mean Transient Duration (µs)	Std. Dev. Transient Duration (µs)	Avg. Pk. Voltage (V)	Std. Dev. Pk Voltage (V)	Min Pk. Voltage (V)	Max Pk Voltage (V)	Mean Abs. Pk. Voltage (V)	Std. Dev. Pk. Voltage (V)
45.9	19800	1.192	1.204	0.000	0.761	-3.316	2.253	0.527	0.549
34.5	19458	1.085	0.870	0.030	0.981	-3.285	2.391	0.794	0.576
29.1	17977	1.067	0.778	0.007	0.925	-3.257	2.090	0.755	0.534
19.3	12257	1.174	0.646	-0.014	0.579	-3.201	1.660	0.489	0.309
8.83	8613	1.287	0.460	-0.018	0.363	-3.137	1.117	0.279	0.219
2.73	463	1.284	0.454	-0.021	0.206	-0.949	0.358	0.089	0.052
1.33	85	1.288	0.448	-0.011	0.195	-0.528	0.229	0.004	0.027

6 Summary

Single-event effects of the INA1H94-SEP radiation-hardened, high common-mode voltage difference amplifier were studied. The device was shown through characterization to be latch-up immune up to surface LET_{EFF} = 43MeV-cm^2 / mg and T = 125°C.

Copyright © 2025 Texas Instruments Incorporated

A Texas A&M University Results Appendix

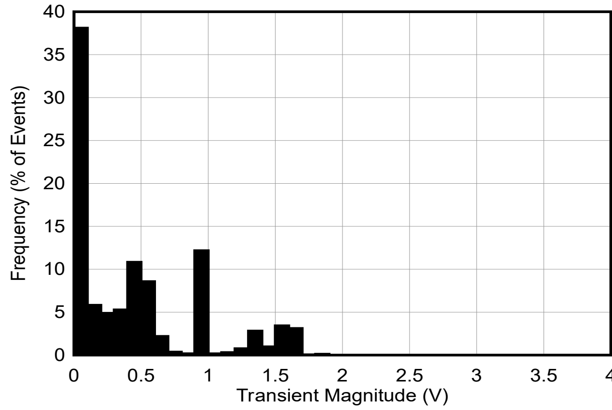

Figure A-1. Transient Event Magnitude Histogram, 5V Supply, LETeff = 45.9MeV-cm^2 / mg

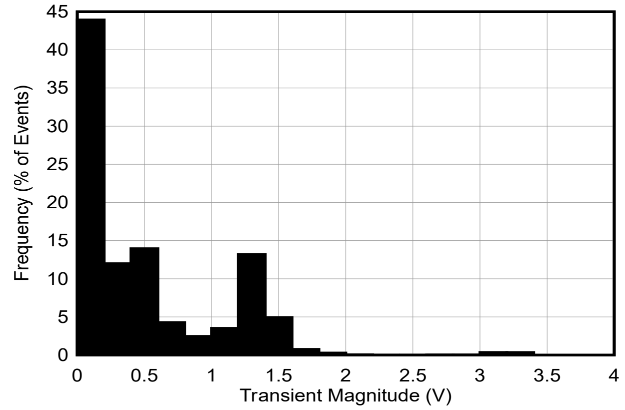

Figure A-2. Transient Event Magnitude Histogram, 18V Supply, LETeff = 45.9MeV-cm^2 / mg

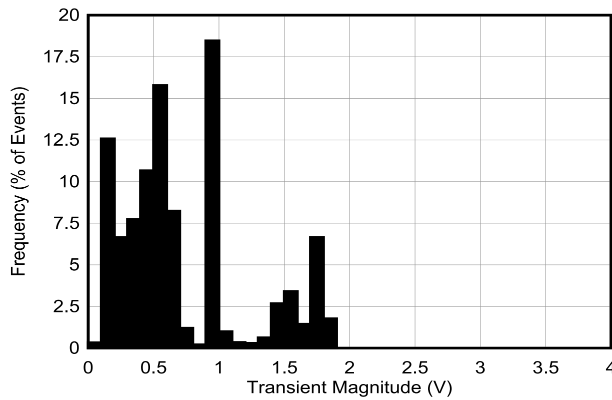

Figure A-3. Transient Event Magnitude Histogram, 5V Supply, LETeff = 34.5MeV-cm^2 / mg

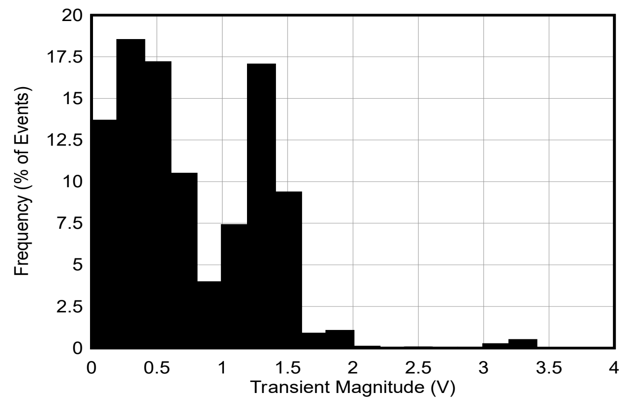

Figure A-4. Transient Event Magnitude Histogram, 18V Supply, LETeff = 34.5MeV-cm^2 / mg

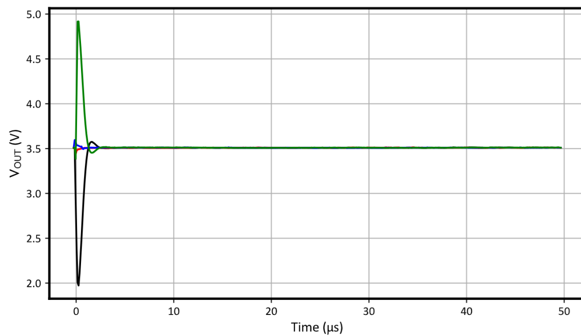

Figure A-5. 18V Supply, LETeff = 45.9MeV-cm^2 / mg, Typical Output Transients

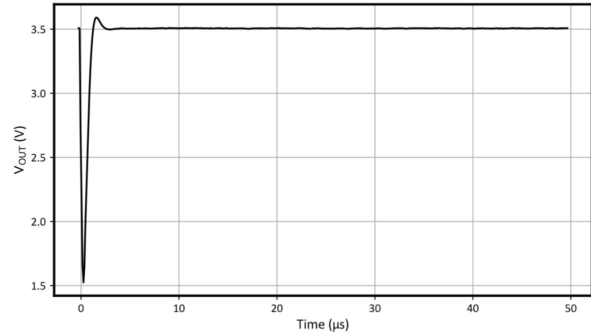

Figure A-6. 18V Supply, LETeff = 45.9MeV-cm^2 / mg, Large Neg Out Transient

Copyright © 2025 Texas Instruments Incorporated

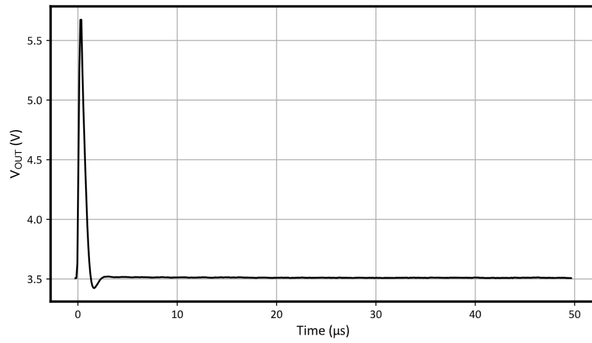

Figure A-7. 18V Supply, LETeff = 45.9MeV-cm^2 / mg, Large Pos Out Transient

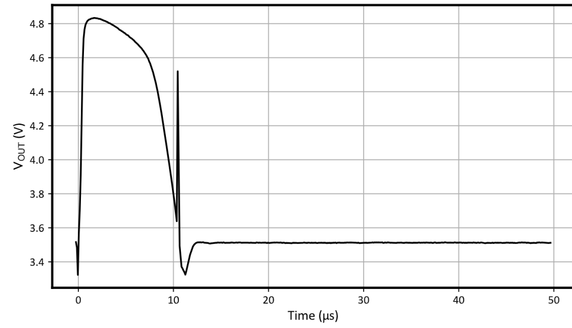

Figure A-8. 18V Supply, LETeff = 45.9MeV-cm^2 / mg, Long Pos Out Transient

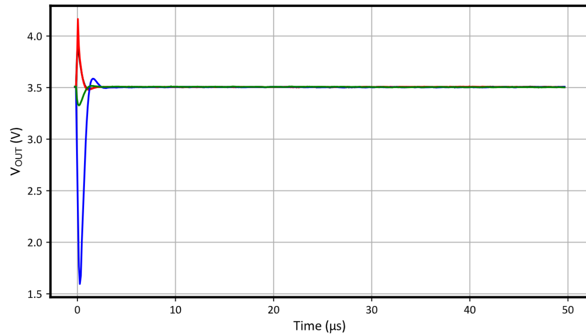

Figure A-9. 18V Supply, LETeff = 34.5MeV-cm^2 / mg, Typical Output Transients

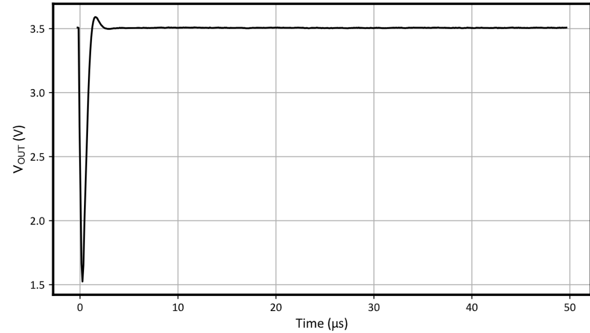

Figure A-10. 18V Supply, LETeff = 34.5MeV-cm^2 / mg, Large Neg Out Transient

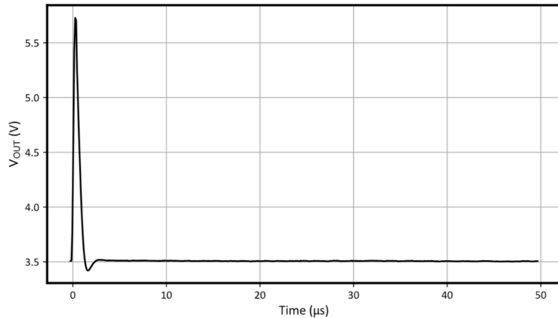

Figure A-11. 18V Supply, LETeff = 34.5MeV-cm^2 / mg, Large Pos Out Transient

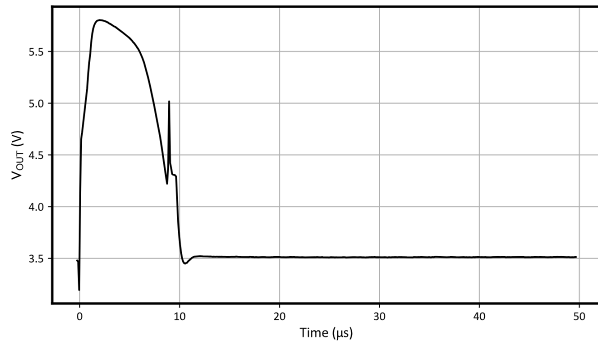

Figure A-12. 18V Supply, LETeff = 34.5MeV-cm^2 / mg, Long Pos Out Transient

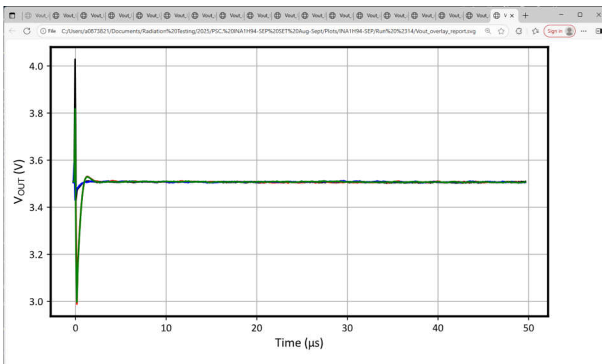

Figure A-13. 18V Supply, LETeff = 29.1MeV-cm^2 / mg, Typical Output Transients

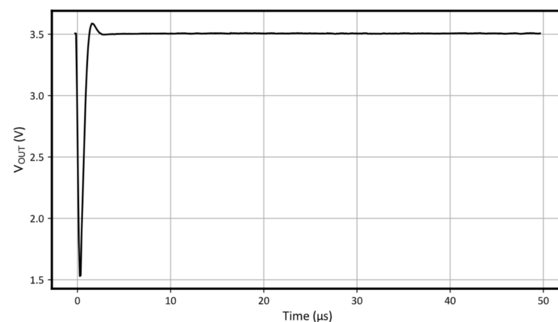

Figure A-14. 18V Supply, LETeff = 29.1MeV-cm^2 / mg, Large Neg Out Transient

Copyright © 2025 Texas Instruments Incorporated

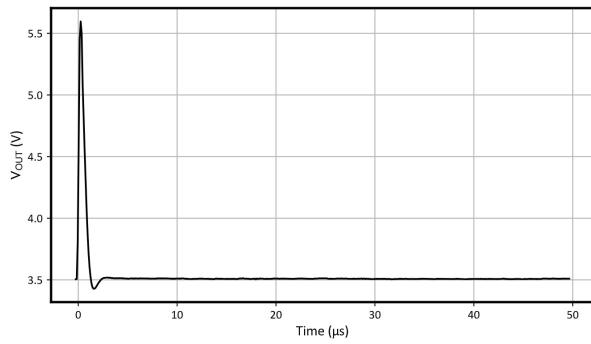

Figure A-15. 18V Supply, LETeff = 29.1MeV-cm^2 / mg, Large Pos Out Transient

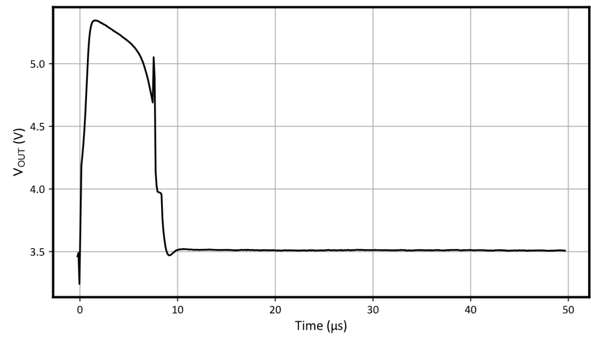

Figure A-16. 18V Supply, LETeff = 29.1MeV-cm^2 / mg, Long Pos Out Transient

Copyright © 2025 Texas Instruments Incorporated

B References

1. M. Shoga and D. Binder, Theory of Single Event Latchup in Complementary Metal-Oxide Semiconductor Integrated Circuits, *IEEE Trans. Nucl. Sci., Vol. 33(6)*, Dec. 1986, pp. 1714-1717.
2. G. Bruguier and J. M. Palau, "Single particle-induced latchup", *IEEE Trans. Nucl. Sci., Vol. 43(2)*, Mar. 1996, pp. 522-532.
3. Texas A&M University, *Texas A&M University Cyclotron Institute Radiation Effects Facility*, webpage.
4. Michigan State University, *MSU Facility for Rare Isotope Beams*, webpage.
5. Ziegler, James F. *The Stopping and Range of Ions in Matter*, webpage.
6. D. Kececioglu, “Reliability and Life Testing Handbook”, Vol. 1, PTR Prentice Hall, New Jersey, 1993, pp. 186-193.
7. Vanderbilt University, *ISDE CRÈME-MC*, webpage.
8. A. J. Tylka, J. H. Adams, P. R. Boberg, et al.,"CREME96: A Revision of the Cosmic Ray Effects on Micro-Electronics Code", *IEEE Trans. on Nucl. Sci., Vol. 44(6)*, Dec. 1997, pp. 2150-2160.
9. A. J. Tylka, W. F. Dietrich, and P. R. Boberg, "Probability distributions of high-energy solar-heavy-ion fluxes from IMP-8: 1973-1996", *IEEE Trans. on Nucl. Sci.,Vol. 44(6)*, Dec. 1997, pp. 2140-2149.

Copyright © 2025 Texas Instruments Incorporated

IMPORTANT NOTICE AND DISCLAIMER

TI PROVIDES TECHNICAL AND RELIABILITY DATA (INCLUDING DATASHEETS), DESIGN RESOURCES (INCLUDING REFERENCE DESIGNS), APPLICATION OR OTHER DESIGN ADVICE, WEB TOOLS, SAFETY INFORMATION, AND OTHER RESOURCES "AS IS" AND WITH ALL FAULTS, AND DISCLAIMS ALL WARRANTIES, EXPRESS AND IMPLIED, INCLUDING WITHOUT LIMITATION ANY IMPLIED WARRANTIES OF MERCHANTABILITY, FITNESS FOR A PARTICULAR PURPOSE OR NON-INFRINGEMENT OF THIRD PARTY INTELLECTUAL PROPERTY RIGHTS.

These resources are intended for skilled developers designing with TI products. You are solely responsible for (1) selecting the appropriate TI products for your application, (2) designing, validating and testing your application, and (3) ensuring your application meets applicable standards, and any other safety, security, regulatory or other requirements.

These resources are subject to change without notice. TI grants you permission to use these resources only for development of an application that uses the TI products described in the resource. Other reproduction and display of these resources is prohibited. No license is granted to any other TI intellectual property right or to any third party intellectual property right. TI disclaims responsibility for, and you fully indemnify TI and its representatives against any claims, damages, costs, losses, and liabilities arising out of your use of these resources.

TI's products are provided subject to TI's Terms of Sale, TI's General Quality Guidelines, or other applicable terms available either on ti.com or provided in conjunction with such TI products. TI's provision of these resources does not expand or otherwise alter TI's applicable warranties or warranty disclaimers for TI products. Unless TI explicitly designates a product as custom or customer-specified, TI products are standard, catalog, general purpose devices.

TI objects to and rejects any additional or different terms you may propose.

Copyright © 2025, Texas Instruments Incorporated

Last updated 10/2025